

# LOCAL NEUTRON STAR MERGER RATE INFERRED FROM THE SHORT GRB DATA AND GRB/GW ASSOCIATION CONTRIBUTED BY OFF-AXIS EVENTS

ZHI-PING JIN<sup>1,2</sup>, XIANG LI<sup>1</sup>, HAO WANG<sup>1,2</sup>, YUAN-ZHU WANG<sup>1,2</sup>, YI-MING HU<sup>3</sup>, HAO-NING HE<sup>1</sup>, QIANG YUAN<sup>1,2</sup>, FU-WEN ZHANG<sup>4</sup>, YUAN-CHUAN ZOU<sup>5</sup>, YI-ZHONG FAN<sup>1,2</sup>, AND DA-MING WEI<sup>1,2</sup>

<sup>1</sup> Key Laboratory of dark Matter and Space Astronomy, Purple Mountain Observatory, Chinese Academy of Science, Nanjing, 210008, China.

<sup>2</sup> School of Astronomy and Space Science, University of Science and Technology of China, Hefei, Anhui 230026, China.

<sup>3</sup> TianQin Research Center for Gravitational Physics, Sun Yat-sen University, Zhuhai, 519082, China.

<sup>4</sup> College of Science, Guilin University of Technology, Guilin 541004, China.

<sup>5</sup> School of Physics, Huazhong University of Science and Technology, Wuhan 430074, China.

## ABSTRACT

Short duration GRBs (SGRBs) are widely believed to originate from neutron star mergers and the merger rate can be estimated via the observed GRB rate with the correction of the outflow half-opening angles. The jet breaks in the afterglow lightcurves of SGRBs, rarely detected so far, are crucial for such an approach. In this work we report the detection of jet decline behaviors in the late optical afterglows of GRB 150424A and GRB 160821B and find  $\theta_j \sim 0.1$  rad. Together with the four events (GRB 051221A, GRB 090426A, GRB 111020A and GRB 130603B) reported before 2015 and the other three “identified” recently (GRB 050709, GRB 060614 and GRB 140903A), we thus have a sample consisting of nine SGRBs (including one long-short event) with a reasonably estimated  $\theta_j$ . In particular, three events in the sample are local (i.e., their redshifts are  $\leq 0.2$ ), with which we can conservatively estimate the local neutron star merger rate density to be  $\sim 130 \text{ Gpc}^{-3} \text{ yr}^{-1}$ , and the real value is likely  $\sim 10$  times higher, suggesting a detection rate  $\sim 60 \text{ yr}^{-1}$  of advanced LIGO/Virgo in their full sensitivity runs. We also show that if the merger-driven relativistic ejecta are structured in a wide solid angle, the prompt emission of some very-nearby (i.e.,  $\leq 200 \text{ Mpc}$ ) off-axis events may be detectable, leading to a GRB/GW association probability of  $\sim 10\%$ .

*Keywords:* gamma-ray burst: individual: GRB 150424A, GRB160821B —binaries: close—gravitational wave

## 1. INTRODUCTION

Gamma-ray Bursts are brief, intense gamma-ray flashes that are widely believed to be powered by the dying massive stars (also called as collapsars) or the merging of the compact binaries involving at least one neutron star (see Piran 2004; Kumar & Zhang 2015, for reviews). Bright supernova (SN) emissions have been detected in the late afterglows of some low-redshift long duration GRBs (LGRBs, i.e., GRBs with durations longer than 2 seconds), established their collapsar origin (Woosley & Bloom 2006). The neutron star merger model is more likely relevant to short GRBs (SGRBs), the events with durations shorter than 2 seconds (Kouveliotou 1993; Eichler et al. 1989). So far, the direct evidence for the merger origin of SGRBs is still absent due to the non-detection of SGRB/GW association. There is, however, some indirect evidence for SGRBs originating from compact binaries, including the location of SGRBs in elliptical galaxies, non-detection of associated SN, large galaxy offsets, weak spatial correlation of SGRBs and star formation regions within their host galaxies (see Nakar 2007; Berger 2014, for reviews), and in particular the identification of the so-called Li-Paczynski macronovae in GRB 130603B (Tanvir et al. 2013; Berger et al. 2013), GRB 060614 (Yang et al. 2015; Jin et al. 2015) and GRB 050709 (Jin et al. 2016). The Li-Paczynski macronova (also called a kilonova) is a new kind of near-infrared/optical transient, powered by the radioactive decay of r-process material, which is synthesized in the ejecta launched during the merger event (e.g., Li & Paczynski 1998; Kulkarni 2005; Metzger et al. 2010; Barnes & Kasen 2013; Tanaka & Hotokezaka 2013). On the other hand, the mergers of compact binaries consisting of neutron stars (NSs) and/or black holes (BHs) are promising sources of gravitational waves (GW; Clark & Eardley 1977). Therefore, SGRBs are expected to be one of the most important electromagnetic counterparts of the GW events (e.g., Eichler et al. 1989; Kochanek & Piran 1993; Li et al. 2016; Baiotti & Rezzolla 2017).

In the pre-GW era, the SGRB data had been widely used to estimate the rate of neutron star mergers and hence the detection prospect of the GW detectors (e.g., Guetta & Piran 2005; Nakar 2007; Abadie et al. 2010; Coward et al. 2012; Fong & Berger 2013; Fong et al. 2014). Such an approach is still necessary in the era of advanced LIGO/VIRGO. This is because, though the

mergers of double neutron stars (neutron star-black hole binaries) can be directly measured by advanced LIGO/Virgo, the horizon distances of detecting such events by the second generation detectors are still limited to be  $z < 0.1$  (0.2) even under the optimistic situation (for example, the successful detection of the electromagnetic counterparts). Therefore, at relatively higher redshifts, the SGRB data are valuable in estimating the neutron star merger rate. At low redshifts, the comparison of the geometry-corrected SGRB rate with the directly measured neutron star merger rate can be used to evaluate the probability of launching relativistic outflow in these mergers. For such purposes, the half-opening angles of the SGRB ejecta are crucial. In principle, the half-opening angle of GRB ejecta can be reasonably estimated with the measured jet break in the afterglow light curve (Rhoads 1999; Sari et al. 1999). Such jet breaks are unfortunately only rarely detected for SGRBs. As summarized in Fong et al. (2015), previously there were just four SGRBs, including GRB 051221A, GRB 090426A, GRB 111020A and GRB 130603B, with reliable jet break measurements and hence the half-opening angle estimates. The deep X-ray measurement of GRB 140903A reveals a jet break at  $\sim 1$  day after the burst (Troja et al. 2016a), suggesting a  $\theta_j \sim 0.05 - 0.1$  rad (Zhang et al. 2017). The sample increases a bit further if we also include the jet break displaying in the so-called long-short GRB (lsGRB) 060614 (Xu et al. 2009; Jin et al. 2015) and the quick decline behavior needed in modeling of short GRB 050709 (Jin et al. 2016). Even so, the “enlarged” sample consists of just  $< 7\%$  SGRBs and it is unclear whether the majority of the SGRBs are beamed or not. One speculation is that the jet breaks usually take place very late and deep follow-up observations are needed. The search for macronova/kilonova components in late time afterglow emission of SGRBs, motivated by the signal detected in GRB 130603B, provided us such a chance. In this work we analyzed the HST data of GRB 150424A (Tanvir et al. 2015) and GRB 160821B (Troja et al. 2016b) to search for the jet breaks as well as the macronova signals.

This work is organized as following. In section 2, we describe our data analysis of GRB 150424A and GRB 160821B, and identify the jet breaks (or more exactly, the post-jet-break decline behavior). We also examine whether there is the evidence for a macronova emission component in GRB 160821B, and estimate the neutron star merger rate density in the local Universe. In section 3, inspired by the narrow jets found in the current sample, we investigate whether the off-beam GRBs (in the uniform jet model) or the off-axis events (in the structured jet model) can significantly contribute to the GRB/GW association or not. We summarize our results with some discussions in section 4.

## 2. DATA ANALYSIS OF GRB 150424A AND GRB 160821B, JET BREAKS OF SGRBS/LSGRB, AND THE LOCAL NEUTRON STAR MERGER RATE

### 2.1. Observations and data analysis of GRB 150424A and GRB 160821B

SGRB 150424A was detected by the Burst Alert Telescope (BAT) onboard *Swift* satellite at 07:42:57 (UT) on April 24, 2015 (Beardmore et al. 2015). The BAT light curve is composed by a bright multi-peaked short episode (start from T-0.05 to T+0.5 second) and a very weak extended emission (lasted to about  $T + 100$  seconds) (Barthelmy et al. 2015). Konus-Wind also detected a multi-peak short burst with total duration of  $\sim 0.4$  second (Golenetskii et al. 2015). At 1.6 hours after the trigger, Keck telescope observed the field and found the optical afterglow (Perley & McConnell 2015). Marshall & Beardmore (2015) checked the earlier *Swift* UV optical telescope (UVOT) observations and found the afterglow, too. Hubble Space Telescope (HST) visited the burst site for three epochs within a month (PI: Nial Tanvir, HST program ID: 13830). Recently, Knust et al. (2017) reported the multi-wavelength observation data of GRB 150424A and interpreted the central engine as a magnetar. Now we focus on the late observations ( $>0.5$  day) to search for possible jet break and the macronova signal.

SGRB 160821B was detected by the *Swift* BAT at 22:29:13 (UT) on August 21, 2016 (Siegel et al. 2016). Its duration is  $T_{90} = 0.48 \pm 0.07$  second. Following the BAT trigger, the X-ray telescope (XRT) and UVOT slew to the burst site immediately and started the observation in 66 and 76 seconds, respectively. The XRT found the afterglow at R.A.=18:39:54.71 Dec.=62:23:31.3 (J2000) with an uncertainty of 2.5 arcseconds (Siegel et al. 2016). Based on the observation started at 0.548 hour after the burst, the Nordic Optical Telescope (NOT) firstly reported the detection of the optical afterglow at R.A.=18:39:54.56 Dec.=62:23:30.5 (J2000) with an uncertainty of 0.2 arcsecond, and a host galaxy candidate which lies at about 5.5" away (Xu et al. 2016). Later, the William Herschel Telescope spectral observations of the host galaxy claimed a redshift of  $z = 0.16$  based on the  $H\alpha$ ,  $H\beta$  and OIII4959/5007Å lines. The unambiguous classification as SGRB and the plausible low redshift make it an ideal candidate to search for a macronova. HST visited the burst site for three epochs within a month (PI: Nial Tanvir, HST program ID: 14237).

Now the HST data of both GRB 150424A and GRB 160821B are publicly-available and we have downloaded these data from the Barbara A. Mikulski Archive for Space Telescopes (MAST: <http://archive.stsci.edu/>). For GRB 150424A, we carry out an independent analysis of HST data in a way slightly different from Knust et al. (2017). We have used image subtraction technique taking all  $t > 20$  days observations as reference images. The afterglow is very weak in the second HST observation epoch. We took a small aperture (3 pixels) for photometry, and then corrected to an infinite aperture. The results are reported in Tab.1 and Tab.2.

GRB 150424A is found near a bright spiral galaxy  $R \sim 20$  mag (Perley & McConnell 2015) at a redshift of  $z = 0.30$  (Castro-

Table 1. Observations of GRB150424A.

Time (days)	Exposure (seconds)	Instrument	Filter	Magnitude <sup>a</sup> (AB)
177.44649	2496	HST+WFC3	F475W	(> 27.4) <sup>b</sup>
6.63693	1800	HST+WFC3	F606W	26.03 ± 0.06
9.22345	1800	HST+WFC3	F606W	26.98 ± 0.14
13.86864	1800	HST+WFC3	F606W	28.03 ± 0.37
178.47184	1800	HST+WFC3	F606W	(> 28.2) <sup>b</sup>
177.51281	2496	HST+WFC3	F814W	(> 26.9) <sup>b</sup>
177.61249	5395	HST+WFC3	F105W	(26.20 ± 0.11) <sup>b</sup>
6.67527	1498	HST+WFC3	F125W	25.25 ± 0.08
9.26352	1498	HST+WFC3	F125W	26.32 ± 0.21
13.92497	1498	HST+WFC3	F125W	27.08 ± 0.42
178.51300	1498	HST+WFC3	F125W	(26.22 ± 0.19) <sup>b</sup>
6.70905	1498	HST+WFC3	F160W	25.08 ± 0.07
9.29904	1498	HST+WFC3	F160W	25.83 ± 0.14
13.96139	1498	HST+WFC3	F160W	27.10 ± 0.44
178.56572	1498	HST+WFC3	F160W	(25.67 ± 0.13) <sup>b</sup>

**Notes.** a. These values have not been corrected for the Galactic extinction of  $A_V = 0.06$  mag.  
b. Quote to the underlying source S1, which lies at about 0.2 second northeast.

Table 2. Observations of GRB 160821B

Time <sup>a</sup> (days)	Exposure (seconds)	Instrument	Filter	Magnitude <sup>b</sup> (AB)	Flux ( $\mu$ Jy)
3.64375	2484	HST+WFC3	F606W	26.00 ± 0.04	0.145 ± 0.006
10.39618	2484	HST+WFC3	F606W	28.0 ± 0.3	0.023 ± 0.006
23.16018	1350	HST+WFC3	F606W	> 27.9 <sup>b</sup>	< 0.025 <sup>b</sup>
103.40406	2484	HST+WFC3	F606W	– <sup>c</sup>	– <sup>c</sup>
3.77481	2397	HST+WFC3	F110W	24.78 ± 0.03	0.445 ± 0.012
10.52723	2397	HST+WFC3	F110W	26.7 ± 0.2	0.076 ± 0.014
23.18086	1498	HST+WFC3	F110W	> 28.0 <sup>b</sup>	< 0.023 <sup>b</sup>
99.26591	5395	HST+WFC3	F110W	– <sup>c</sup>	– <sup>c</sup>
3.70861	2397	HST+WFC3	F160W	24.50 ± 0.04	0.575 ± 0.019
10.46105	2397	HST+WFC3	F160W	26.9 ± 0.3	0.063 ± 0.018
23.23040	2098	HST+WFC3	F160W	> 27.0	< 0.058

a. These values have not been corrected for the Galactic extinction of  $A_V = 0.04$  mag.  
b. Images have been combined with later exposures as references.  
c. Images have been combined to earlier exposures as references.

Tirado et al. 2015). However, the deep HST observations found that the field of GRB 150424A is very complicated (Tanvir et al. 2015). There is an extended source to the south-west of afterglow (see Fig.1, marked as S1), which could be the host galaxy of GRB 150424A, too. It has been detected in HST F105W, F125W and F160W bands, but not in HST F475W, F606W and F814W bands, see Fig.2. If the break between F105W and F814W is due to the 4000Å break, then the redshift is  $z \sim 1.2$ . While there is no strong evidence for a Lyman break in the Swift UVOT afterglow data (Marshall & Beardmore 2015; Knust et al. 2017), indicating a redshift of  $z \leq 1.0$ . Considering these uncertainties, we suggest that  $z = 0.3$  is favored while  $z \sim 1$  is still possible.

GRB 160821B is also located near a bright ( $R \sim 19.2$  mag) spiral galaxy (Xu et al. 2016), at a redshift of  $z = 0.16$  (Levan et al. 2016). Deep HST observations found no secure detection of any underlying sources near the afterglow (see Fig.3). We then adopt  $z = 0.16$  for this burst.

## 2.2. Identification of the post-jet-break decline behaviors of GRB 150424A and GRB 160821B

In the GRB jet model (see Tab.1 of Zhang & Meszaros (2004) for a comprehensive summary), the afterglow lightcurve declines as  $t^{-p}$  (or slightly shallow if the sideways expansion of the ejecta is ignorable), as long as the ejecta has been decelerated to a bulk Lorentz factor  $\leq 1/\theta_j$ , no matter whether the observer’s frequency  $\nu_{\text{obs}}$  is between  $\nu_m$  and  $\nu_c$  (the spectrum is  $\propto \nu^{-(p-1)/2}$ ) or

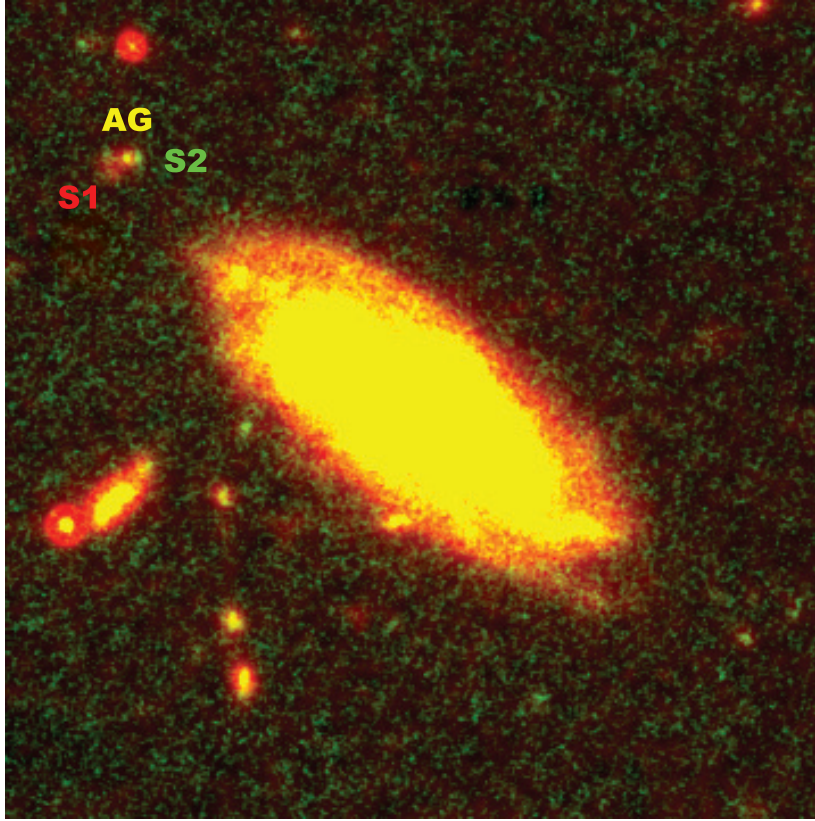


**Figure 1.** False color image of the field of GRB 150424A, which has been converted to north up and east left. Here all HST WFC3 UVIS (including 2496 seconds in F435W, 7200 seconds in F606W and 2496 seconds in F814W) signals appear green and all HST WFC3 IR (including 5395 seconds in F105W, 5991 seconds in F125W and 5991 seconds in F160W) appear red. The afterglow detected in both UV and IR images are marked as AG. There are a red source in the south west only detected in IR images (marked as S1) and a blue source in the east only detected in UV images (marked as S2).

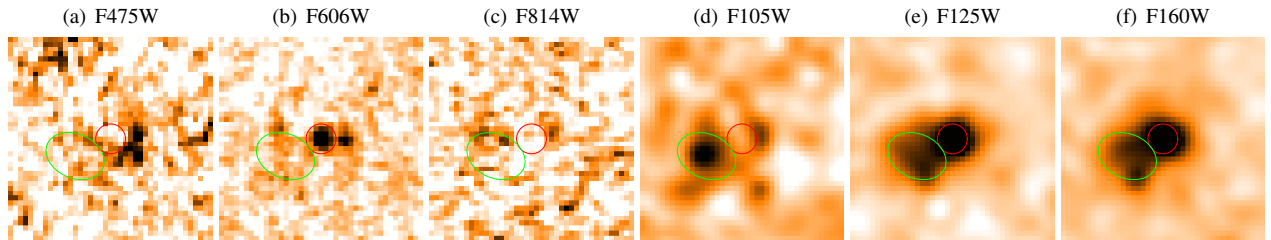


**Figure 2.** The HST observations of GRB 150424A. Each image shows the combined data of all observations in the given filter. The red circle is the position of the afterglow and the green circle is the position of S1.

above both of them (the spectrum is  $\propto \nu^{-p/2}$ ). Therefore, the quick decline  $t^{-\alpha}$  at late time, together with a reliable spectral index which is close to  $(\alpha - 1)/2$  or  $\alpha/2$  for  $\alpha \gtrsim 2$ , are widely taken as the strong evidence for the post-jet-break decline behavior.

For GRB 150424A, the HST near-infrared/F606W afterglow emission dropped with time as  $t^{-2.52 \pm 0.14}$ . If interpreted as the post-jet-break decline, we have  $p \sim 2.5$  and the near-infrared/F606W spectrum should be  $\propto \nu^{-0.75}$  (for  $\nu_m < \nu_{\text{obs}} < \nu_c$ ) or  $\nu^{-1.25}$  (for  $\nu_{\text{obs}} > \max\{\nu_m, \nu_c\}$ ). The measured one is  $\nu^{-0.81 \pm 0.05}$ , which supports the jet break interpretation. Interestingly, the X-ray lightcurve is also consistent with a sharp decline at late times. We therefore suggest a jet break in the late afterglow of GRB 150424A at the time of  $\sim 3.8$  days (see Fig.4).

For GRB 160821B, the publicly-available data are rather limited. The HST observations started at 3.6 days after the burst. Since then the F606W/near-infrared emission dropped with the time as  $\propto t^{-1.9 \pm 0.1}$ . The F606W/near-infrared emission spectrum is  $\propto \nu^{-1.30 \pm 0.05}$  at  $\sim 3.6$  days and  $\propto \nu^{-1.0 \pm 0.2}$  at  $\sim 10.4$  days. These results are reasonably consistent with the afterglow for  $p \sim 2$

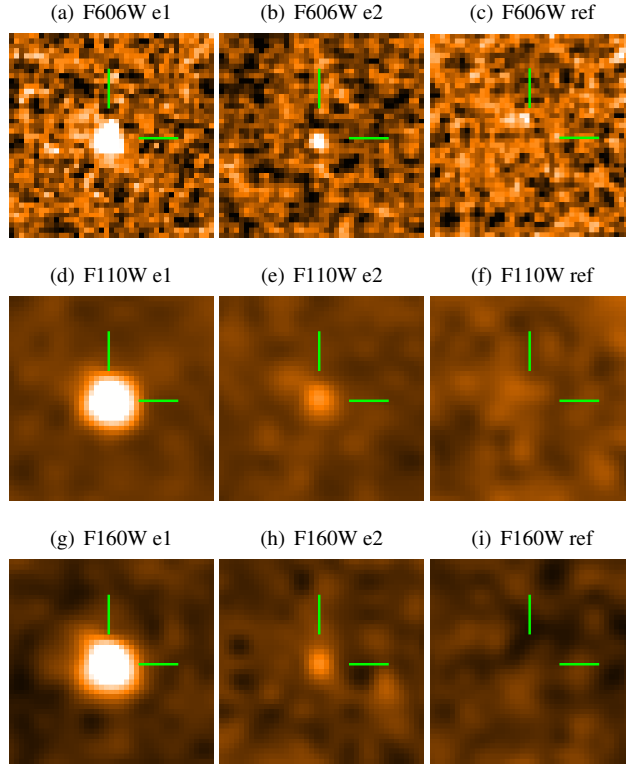


**Figure 3.** The HST observations of GRB 160821B. The afterglow emission were detected in all bands in the first two epochs of observations, and faded away in later epochs. In the images of the last epoch, which we take as references, no source is reliably detected near the afterglow position.

(or slightly larger supposing the sideways expansion of the ejecta is unimportant, as found in the numerical calculations) and  $\nu_{\text{obs}} > \max\{\nu_m, \nu_c\}$ . The X-ray afterglow emission in the time interval of  $\sim 0.05 - 2$  day after the burst also strongly indicate the presence of a jet break at  $t \geq 0.3$  day. The analytical approach yields a  $t_{\text{jet}} \sim 0.7$  day (see Fig.6).

With the break time, the jet half-opening angle can be estimated by (Sari et al. 1999; Frail et al. 2001)

$$\theta_j \approx 0.076 \left( \frac{t_{\text{jet}}}{1 \text{ day}} \right)^{3/8} \left( \frac{1+z}{2} \right)^{-3/8} \left( \frac{E_{\text{iso}}}{10^{51} \text{ erg}} \right)^{-1/8} \left( \frac{\eta_\gamma}{0.2} \right)^{1/8} \left( \frac{n}{0.01 \text{ cm}^{-3}} \right)^{1/8}. \quad (1)$$

For GRB 150424A, Konus-Wind recorded a total gamma-ray (20 keV–10 MeV) fluence of  $1.81 \pm 0.11 \times 10^{-5} \text{ erg cm}^{-2}$  (Golenetskii et al. 2015), corresponding to an isotropic gamma-ray emission energy of  $E_{\text{iso}} \sim 4.3 \times 10^{51}$  or  $\sim 1.0 \times 10^{53}$  erg at  $z = 0.3$  or 1.0, respectively, using cosmological parameters of Planck results (Planck Collaboration 2014). The Fermi gamma-ray (10–1000 keV) fluence is  $1.68 \pm 0.19 \times 10^{-6} \text{ erg cm}^{-2}$  for GRB 160821B (Stanbro et al. 2016), so we have  $E_{\text{iso}} \sim 10^{50}$  erg for  $z = 0.16$ . Following Frail et al. (2001) we take the radiation efficiency  $\eta_\gamma = 0.2$ . For the ISM number density  $n = 0.01 \text{ cm}^{-3}$  (see Fong et al. 2015 for the evidence of the low number density of the ISM surrounding SGRBs), we get  $\theta_j \approx 0.12$  for GRB 150424A (if we take  $z = 1.0$  then  $\theta_j \sim 0.07$ ) and  $\theta_j \approx 0.11$  for GRB 160821B.

A reliable jet half-opening angle has only been rarely inferred for SGRBs/lsGRBs (Please see Tab.3 for a summary). Interestingly, all low-redshift ( $z \leq 0.4$ ) events (except GRB 050502B, of which the optical afterglow emission was never detected) with deep HST follow-up observations are in this sample. These events include GRB 050709, GRB 060614, GRB 130603B, GRB 150424A and GRB 160821B (Note that for GRB 050709, no jet break was directly measured. But the presence of a macronova signal strongly favors a jet break at  $t \leq 1.4$  days after the burst, see Jin et al. 2016). Such an observational fact likely points towards the presence of jet break in most events and their non-detection may simply due to the lack of deep follow-up observations. The other interesting feature is the “narrow” distribution of these estimated  $\theta_j$  that peaks at  $\sim 0.1$  rad, indicating that many more SGRBs/lsGRBs were off-beam (or off-axis).

### 2.3. Any macronova signal in GRB 150424A and/or GRB 160821B?

Table 3. Short/lsGRBs with a jet break (or upper limit).

GRB	$z$	$E_{\text{iso}}$ ( $10^{51}$ erg)	$t_{\text{jet}}$ (days)	$\theta_j$ (rad)	References
050709	0.16	0.07	< 1.4	< 0.14	(1)
051221A	0.546	2.4	5	0.09	(2)
060614	0.125	2.5	1.4	0.08	(3)
090426A	2.609	4.2	0.4	0.08-0.12	(4)
111020A	–	0.21/1.9 <sup>a</sup>	2	0.05-0.14	(5)
130603B	0.356	2.1	0.47	0.07-0.14	(6,7)
140903A	0.351	0.06	1.2	0.05-0.1	(8, 9)
150424A	0.30	4.3	3.8	0.12	this work
160821B	0.16	0.1	0.7	0.11	this work

a. The isotropic-equivalent prompt emission energy was roughly estimated in (5) by assuming different redshifts and physical parameters. References: (1) [Jin et al. \(2016\)](#); (2) [Soderberg et al. \(2006\)](#); (3) [Xu et al. \(2009\)](#); (4) [Nicuesa Guelbenzu et al. \(2011\)](#); (5) [Fong et al. \(2012\)](#); (6) [Fong et al. \(2014\)](#); (7) [Fan et al. \(2013\)](#); (8) [Troja et al. \(2016a\)](#); (9) [Zhang et al. \(2017\)](#).

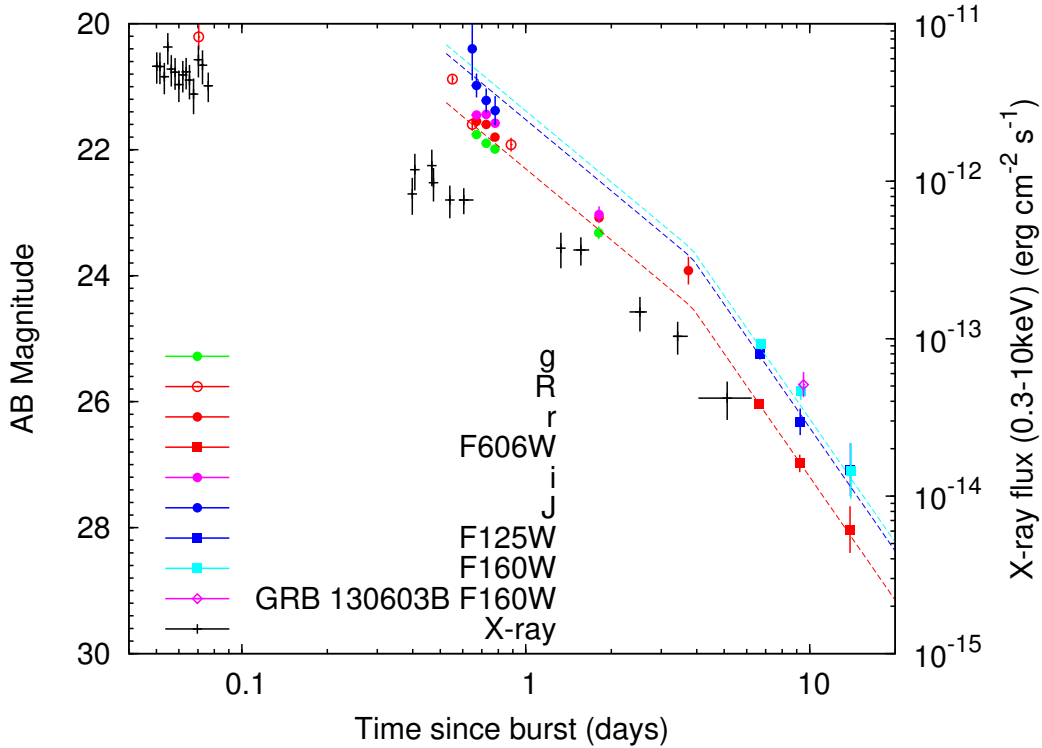


**Figure 4.** The multi-band afterglow lightcurves of GRB 150424A. The early optical data are taken from [Knust et al. \(2017\)](#), the HST data are analyzed in this work, and the *Swift* XRT lightcurve is provided by the UK *Swift* Science Data Centre ([Evans et al. 2009](#)).

For GRB 150424A, based on our analysis of HST data, both the temporal and spectral behaviors are well consistent with the afterglow model and there is no macronova signal, see Fig.4 and Fig.5.

As for GRB 160821B, the situation is less clear. The HST measured data at  $t \sim 3.6$  days after the trigger can be interpreted as the superposition of a power-law afterglow component and a thermal-like component at a temperature of  $\sim 3000$  K. As already noticed by [Troja et al. \(2016b\)](#), the macronova signal, if any, should be 5 times dimmer than that is detected for example in GRB 130603B and might indicate a double neutron star merger origin. Though such a possibility is intriguing, with the current publicly-available data we can not identify a component significantly in excess of the power-law decline afterglow (as the case of GRB 130603B), or a very-significant spectral softening (as the case of GRB 060614), or the obvious chromatic declines in optical/near-infrared bands (as the case of GRB 050709). We thus conclude that more data are needed to clarify whether there is a macronova signal accompanying GRB 160821B or not.

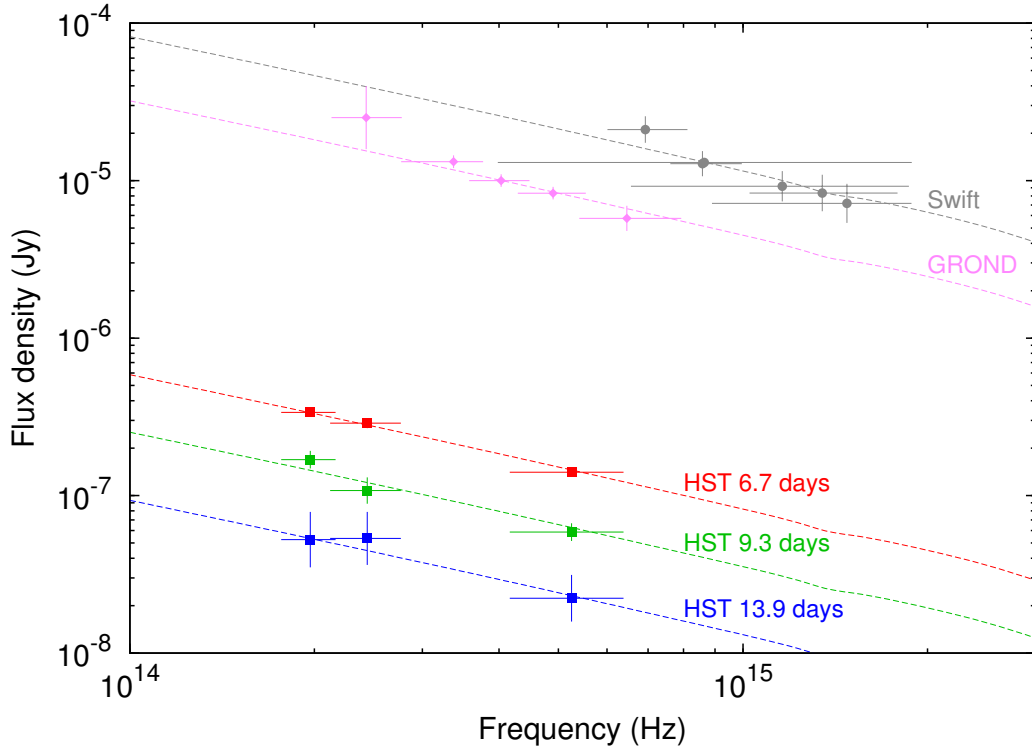


**Figure 5.** The optical SED of the afterglow of GRB 150424A and the fit of a power-law spectrum with extinction of the Galaxy. The *Swift* UVOT data are adopted from [Marshall & Beardmore \(2015\)](#), the GROND data are taken from [Kann et al. \(2015\)](#), and the HST data are analyzed in this work.

#### 2.4. The neutron star merger rate in the local ( $z \leq 0.2$ ) Universe

The SGRB-data based neutron star merger rate was widely estimated in the literature (e.g., [Guetta & Piran 2005](#); [Nakar 2007](#); [Coward et al. 2012](#); [Fong & Berger 2013](#); [Fong et al. 2015](#)). Different from these previous works, benefited from the reasonable estimate of  $\theta_j$  for GRB 050709, GRB 060614 and GRB 160821B, below we estimate the neutron star merger rate, which is a function of the redshift, in the local ( $z \leq 0.2$ ) Universe that can be directly tested by (compared to) the ongoing advanced LIGO/Virgo observations.

GRB 050709 was detected by HETE-II with a field of view F.o.V  $\approx 3$  sr ([Villasenor et al. 2005](#)), while GRB 060614 and GRB 160821B were recorded by *Swift* satellite with a F.o.V  $\approx 2.4$  sr ([Gehrels et al. 2006](#); [Siegel et al. 2016](#)). Note that HETE-II has a much lower detection rate of SGRBs in comparison with *Swift* due to the relatively small effective area of the onboard detector. Moreover, no GRBs were reported by HETE-II any longer since March 2006 (<http://space.mit.edu/HETE/Bursts/>). For simplicity we ignore the difference between HETE-II and *Swift* (see also [Li et al. 2017](#)). The *rate density* of neutron star merger can be calculated via

$$\mathcal{R}_{\text{nsm}} = \frac{N_{\text{event}}}{V(z \leq 0.2) T} \frac{4\pi}{\text{F.o.V}} \frac{1}{1 - \cos \theta_j} \approx 130_{-59}^{+86} \text{ Gpc}^{-3} \text{ yr}^{-1} \left( \frac{\theta_j}{0.1 \text{ rad}} \right)^{-2} \frac{N_{\text{event}}}{3} \left( \frac{T}{11 \text{ yr}} \right)^{-1} \left( \frac{\text{F.o.V}}{2.4 \text{ sr}} \right)^{-1}, \quad (2)$$

where  $N_{\text{event}}$  is the total number of SGRBs/lSGRBs with a reasonably estimated  $\theta_j$  at  $z \leq 0.2$ ,  $T$  is the observation time ( $\approx 11$  years since the SGRBs were firstly localized in 2005) and  $V(z \leq 0.2)$  is the comoving volume.

Please note that eq.(2) is a *very conservative* estimate for three reasons. Firstly, there are three “local” SGRBs (i.e., GRB 061201, GRB 080905A and GRB 150101B) that have not been taken into account due to the lack of enough afterglow data ([Fong et al. 2015](#)). Secondly, there are only  $\leq 1/4$  of SGRBs with a reliable redshift ([Berger 2014](#)) and some other SGRBs could be nearby<sup>1</sup>. For example, recently [Siellez et al. \(2016\)](#) claimed that GRB 070923, 090417A and 131004A were at  $z < 0.1$ . Finally, probably only a fraction of neutron star mergers can produce either SGRBs or lsGRBs. Taking into account these factors, the real

<sup>1</sup> For the local merger-driven GRBs, the situation will change dramatically in the GW era since the gravitational wave data alone can yield reliable luminosity distance and hence the missing  $z$  problem will be solved. The intense deep followup observations of the GW/GRB events are also extremely helpful in measuring the jet breaks of the afterglows.

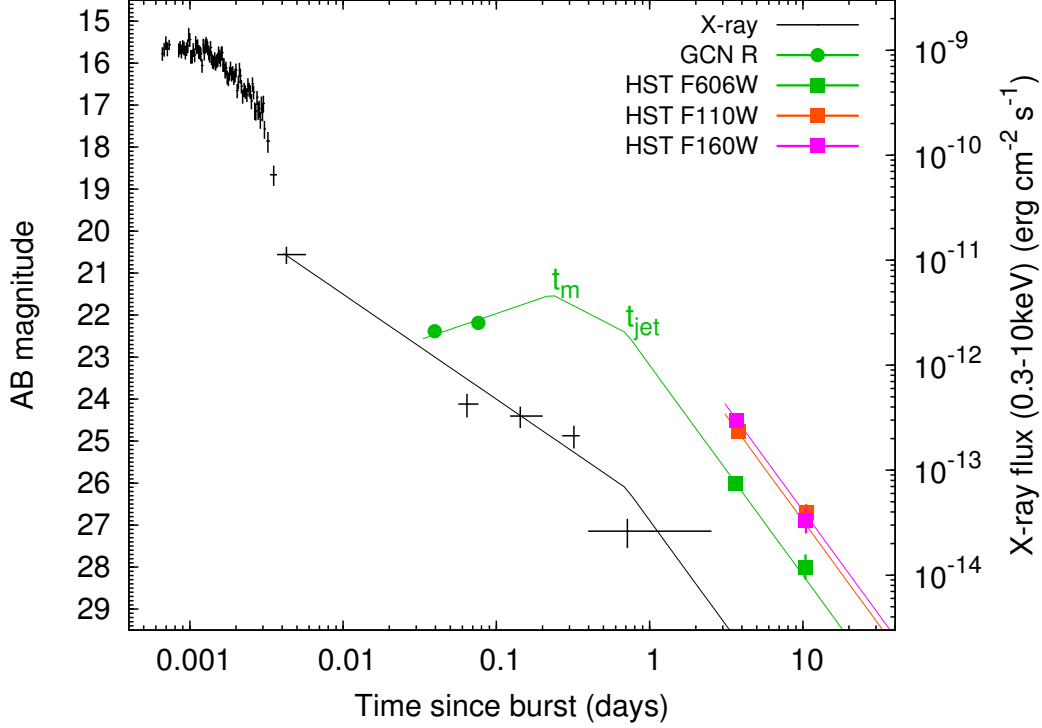


**Figure 6.** The multi-band afterglow lightcurves of GRB 160821B. The *Swift* XRT lightcurve is provided by the UK *Swift* Science Data Centre (Evans et al. 2009). The black and green lines represent the analytic “interpretation” of the afterglow emission. The forward shock emission was in the slow cooling phase and the spectral index of the accelerated electrons ( $p$ ) is about 2. For  $t < t_m$ , the R-band is below  $\nu_m$  and the flux increases with the time as  $t^{1/2}$ . At  $t = t_m$ , R-band crossed  $\nu_m$ , then the flux drops with the times as  $t^{-3(p-1)/4}$ . At  $t > t_{jet}$ , the flux declines as  $t^{-p}$  (the spectra at  $t \geq 3.6$  days however suggest that at late times the optical bands are below both  $\nu_m$  and  $\nu_c$ ). As for the X-ray emission, the observer’s frequency is above both  $\nu_m$  and  $\nu_c$ , and the decline is  $\propto t^{-(3p-2)/4}$  for  $t < t_{jet}$  and  $\propto t^{-p}$  for  $t > t_{jet}$ .

neutron star merger rate density may be enhanced by a factor of  $f_c \sim 10$ . Including such a correction factor we have

$$\mathcal{R}_{\text{nsm}} \approx 1300_{-590}^{+860} \text{ Gpc}^{-3} \text{ yr}^{-1} \frac{f_c}{10} \left( \frac{\theta_j}{0.1 \text{ rad}} \right)^{-2} \frac{N_{\text{event}}}{3} \left( \frac{T}{11 \text{ yr}} \right)^{-1} \left( \frac{\text{F.o.V}}{2.4 \text{ sr}} \right)^{-1}, \quad (3)$$

which is consistent with the “reasonable” estimate of the neutron star merger rate (Abadie et al. 2010) and in agreement with the constraints set by the O1 run data of advanced LIGO (Abbott et al. 2016).

The advanced LIGO detectors can detect the gravitational wave radiation from neutron star mergers within a typical (i.e., direction/inclination averaged) distance  $D \sim (220, 400)$  Mpc (for double neutron star system and  $1.4 - 10M_\odot$  neutron star-black hole system, respectively) at its designed sensitivity (Abadie et al. 2010). The neutron star merger *detection* rate is thus

$$R_{\text{gw,nsm}} \sim 58_{-26}^{+38} \text{ yr}^{-1} \frac{f_c}{10} \left( \frac{\theta_j}{0.1 \text{ rad}} \right)^{-2} \frac{N_{\text{event}}}{3} \left( \frac{D}{220 \text{ Mpc}} \right)^3 \left( \frac{T}{11 \text{ yr}} \right)^{-1} \left( \frac{\text{F.o.V}}{2.4 \text{ sr}} \right)^{-1}. \quad (4)$$

Notice that the above number assumes a perfect GW detector, an realistic one operates with a duty cycle and in reality the expected value would decrease by the coincident duty cycle. Nevertheless, the detection prospect should be quite promising.

### 3. GRB/GW ASSOCIATION: THE CONTRIBUTION OF OFF-AXIS EVENTS

The energy distribution of the GRB ejecta is still unclear. In the standard fireball afterglow model, a conical jet with a uniform energy distribution within the cone and sharp energy depletion at the jet edge are assumed (i.e.,  $\epsilon(\theta) = \epsilon_0$  for  $\theta \leq \theta_j$  otherwise equals to 0, where  $\epsilon(\theta)$  denotes the energy distribution of the ejecta as a function of the polar angle  $\theta$ ). To account for the diverse prompt/afterglow emission of LGRBs, it is further proposed that a non-uniform distribution of energy per solid angle within the jet (i.e., the jets are structured) and the widely-discussed scenarios include (a) the power-law distribution model  $\epsilon(\theta) = \epsilon_0 \theta^{-2}$  for  $\theta > \theta_c$  (Rossi et al. 2002; Zhang & Meszaros 2002; Dai & Gou 2001) otherwise  $\epsilon(\theta) = \epsilon_0$ ; (b) the Gaussian-type jet



$\epsilon(\theta) = \epsilon_0 \exp(-\theta^2/2\theta_c^2)$  (Zhang et al. 2004), which is illustrated in Fig.7 for  $\theta_c \sim 7$  deg and  $\epsilon_0 = 10^{51}$  erg; (c) the two component jet model (Berger et al. 2003; Wu et al. 2005; Huang et al. 2006). The SGRB outflows are likely structured, too, as found in the numerical simulations (Aloy et al. 2005; Murguia-Berthier et al. 2017) and in the afterglow modeling (Jin et al. 2007).

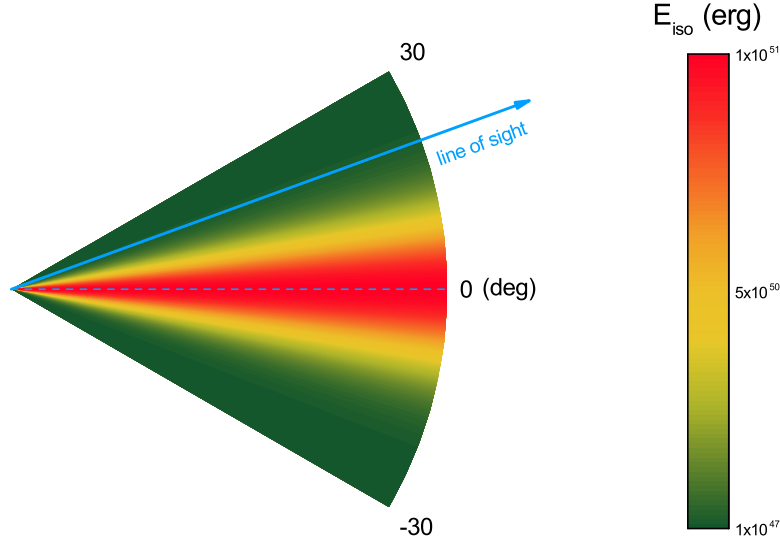


**Figure 7.** Illustration of our off-axis scenario in the structured jet model.

A bright SGRB has a typical isotropic-equivalent kinetic energy of  $E_{\text{iso}} \sim 10^{51}$  erg (Zhang et al. 2012; Fong et al. 2015). Such energetic outbursts are detectable for *Swift* and Fermi-GBM like detectors<sup>2</sup> at a distance of  $D \leq 200$  Mpc even when our line of sight is “slightly” outside of the ejecta (note that in this paragraph we adopt *the uniform jet model*), i.e., the viewing angle  $\theta_v = \theta_j + \Delta\theta$  and the  $\Delta\theta$  satisfies

$$\Delta\theta \leq 0.04 \left[ \frac{E_{\text{iso}}}{10^{51} \text{ erg}} \right]^{1/6} \left( \frac{\eta}{100} \right)^{-1} \left( \frac{D}{200 \text{ Mpc}} \right)^{-1/3} \left( \frac{\mathcal{F}_{\text{th}}}{10^{-7} \text{ erg cm}^{-2}} \right)^{-1/6}, \quad (5)$$

where  $\eta$  is the initial Lorentz factor of the GRB outflow and  $\mathcal{F}_{\text{th}} \sim 10^{-7} \text{ erg cm}^{-2}$  is the fluence threshold for a reliable detection of a weak GRB. The  $\eta$  has been normalized to  $\sim 100$ , motivated by the Lorentz factor–luminosity correlation of GRBs (Lü et al. 2012; Liang et al. 2010; Fan et al. 2012). Unless  $\eta \leq 50$ , we have  $\Delta\theta < \theta_j (\sim 0.1)$ , implying that in the uniform jet model, the off-beam events can enhance the GRB/GW association at most moderately (the enhancement factor is estimated as  $\mathcal{R} \approx (\theta_j + \Delta\theta)^2 / \theta_j^2$ ). Such events should be observed mainly in X-rays and last longer, since the energy of the gamma-rays is lowered by a factor of  $a_0 = [1 + (\eta\Delta\theta)^2]^{-1}$  and the duration is extended by a factor of  $a_0^{-1}$ .

*In the structured jet model*, GRB/GW associations may be more common. In the numerical simulations, relativistic outflows with  $\eta \geq 10$  and  $\epsilon(\theta \leq \theta_{\text{cut}}) \geq 10^{48}$  erg are found within the polar angle of  $\theta_{\text{cut}} \lesssim 0.3 - 0.4$  rad (Aloy et al. 2005; Gottlieb et al. 2017; Murguia-Berthier et al. 2017). The photospheric radius of a relativistic outflow reads  $R_{\text{ph}} \approx 4 \times 10^{11} \text{ cm} (L_{\text{tot}}/10^{48} \text{ erg s}^{-1})(\eta/10)^{-3}$ , where  $L_{\text{tot}}$  is the total luminosity of the outflow (Paczynski 1990). The initial radius of the “reborn” fireball is  $R_0 \sim 10^9 \text{ cm}$  (Aloy et al. 2005). As long as  $R_{\text{ph}}$  is in the same order of  $\eta R_0$ , the thermal radiation will be efficient, requiring that

$$\eta \sim 25 (L_{\text{tot}}/10^{48} \text{ erg s}^{-1})^{1/4} (R_0/10^9 \text{ cm})^{-1/4}. \quad (6)$$

In such a case, the temperature of the emission can be estimated as  $T_{\text{obs}} \sim 20 \text{ keV} (L_{\text{tot}}/10^{48} \text{ erg s}^{-1})^{1/4} (R_0/10^9 \text{ cm})^{-1/2}$ . The

<sup>2</sup> Fermi-GBM like detectors are benefited for their very wide field of view (Meegan et al. 2009), which is very important for establishing the GRB/GW association. *Swift* actually has a much higher sensitivity but the field of view is just  $\sim 2.4$  sr.

corresponding peak energy of the observed spectrum ( $\nu f_\nu$ ) is thus

$$E_p \sim 3.92T_{\text{obs}} \sim 78 \text{ keV} (L_{\text{tot}}/10^{48} \text{ erg s}^{-1})^{1/4} (R_0/10^9 \text{ cm})^{-1/2}, \quad (7)$$

where the redshift correction has been ignored since in this work we concentrate on the nearby events. The emission duration is likely determined by the width of the ejecta in the direction of the line of sight. Such emission, if within a distance of  $\sim 200$  Mpc, are detectable for *Swift* and Fermi-GBM like detectors. The association chance between these weak GRB-like transients and GW events is larger than that between the bright SGRBs and GW events by a factor of

$$\mathcal{R} \sim \frac{1 - \cos \theta_{\text{cut}}}{1 - \cos \theta_j} \sim 16 \frac{(\theta_{\text{cut}}/0.4 \text{ rad})^2}{(\theta_j/0.1 \text{ rad})^2}, \quad (8)$$

implying a more promising prospect of establishing the GRB/GW association in the near future. The other prediction of the off-axis ejecta model is an unambiguous re-brightening of the afterglow due to the emergence of the forward shock emission of the energetic ejecta core (Wei & Jin 2003; Kumar & Granot 2003). Since the beam-corrected SGRB rate (see eq.(2) and eq.(3)) is already comparable to the population synthesis prediction of the neutron star mergers (Dominik et al. 2015), it is reasonable to speculate that SGRBs were produced in a good fraction of mergers, for which the GRB/GW association probability may be as high as  $\sim \theta_{\text{cut}}^2/2 \sim 10\%$ . The prospect of establishing the GRB/GW association is thus more promising than that suggested in the literature (Williamson et al. 2014; Clark et al. 2015; Li et al. 2016).

Very recently, Lazzati et al. (2017) calculated the emission from the possible wide cocoon (i.e., within the polar angle  $\sim 40^\circ$ ) surrounding the SGRB outflow and suggested the prompt X-ray emission with  $E_{\text{iso}} \sim 10^{49}$  erg, which is significantly stronger than our signal. Such kind of energetic shortly-lasting X-ray outbursts will be nice electromagnetic counterparts of GW events (see however Gottlieb et al. 2017, for the results based on the 3 dimensional simulation).

In the above discussion, the successful launching of GRB ejecta is assumed. This may be not always the case. As already revealed by the numerical simulations, some relativistic ejecta can not break out successfully if the initial half-opening angles are too wide (see e.g. Aloy et al. 2005; Nagakura et al. 2014; Murguia-Berthier et al. 2017). In such cases, low luminosity events may be powered by the mildly-relativistic outflow. The simple thermal radiation model, however, is usually unable to give rise to significant emission at energies above 10 keV for  $\eta \leq 10$  (not that as long as  $R_{\text{ph}} \gg \eta R_0$ , we have  $E_p \propto \eta^{8/3}$ ) and additional physical process(es) (e.g., magnetic energy dissipation) should be introduced to generate X-ray/gamma-ray emission.

#### 4. SUMMARY AND DISCUSSION

After the discovery of the SGRB afterglow, dedicated efforts have been made to identify the jet breaks and then infer the half-opening angles. However, the sample increases rather slowly due to the dim nature of these events. The main reason for the non-detection/identification of the jet breaks in most SGRB afterglows may be the lack of deep follow-up observations. The realization that the macronovae may appear within one to two weeks after the GRBs inspired the very late afterglow observations. With these high-quality optical/near-infrared data we found two jet breaks in GRB 150424A and GRB 160821B. Together with the previous results, we have a SGRB/jet sample consisting of nine events (including one long-short event). The inferred half-opening angles have a very narrow distribution (i.e.,  $\theta_j \sim 0.1$ ). Though the sample is still small, there are three events taking place locally (i.e.,  $z \leq 0.2$ ), with which the ‘‘local’’ neutron star merger rate density has been estimated to be  $\sim 130 \text{ Gpc}^{-3} \text{ yr}^{-1}$ . Such a SGRB-based local neutron star merger rate, however, is rather conservative since a few ‘‘local’’ SGRBs (including GRB 061201, GRB 080905A and GRB 150101B) have not been taken into account, and moreover just  $\sim 1/4$  SGRBs have redshifts. Further enhancement is plausible if the SGRB production fraction of neutron star mergers is considerably lower than 100%. Taking into account all these uncertainties, the local neutron star merger rate can be as high as  $\gtrsim 10^3 \text{ Gpc}^{-3} \text{ yr}^{-1}$ , implying a very promising detection prospect of advanced LIGO/Virgo.

We have also examined the HST data of GRB 150424A and GRB 160821B to search for possible macronova signal(s). In GRB 150424A no sign has been found. While in GRB 160821B, the HST and Keck (Kasliwal et al. 2017) data at  $t \sim 3.7 - 4.3$  days can be interpreted as a power-law afterglow component plus a thermal component at a temperature of  $\sim 3000$  K. However, with the currently rather-limited (publicly-)available data, no evidence as strong as that for GRB 130603B, GRB 060614 and GRB 050709 can be provided.

Finally, motivated by the plausible promising detection prospect of neutron star mergers in the near future, we have re-estimated the GRB/GW association probability. For the very nearby (i.e.,  $D \leq 200$  Mpc) events, some off-beam GRBs (in the uniform jet model) may be detectable, possibly appearing as the low-luminosity X-rich transients/GRBs (lasting  $\sim 1 - 10$  s). The enhancement of the GRB/GW association is, however, at most moderate. The situation is different if the merger-driven relativistic ejecta are structured in a wide solid angle. In such a case, the prompt emission of the relativistic ejecta, though viewed off-axis, are detectable for *Swift* and Fermi-GBM like detectors if the sources are at  $D \leq 200$  Mpc and the corresponding GRB/GW association probability may be high up to  $\sim 10\%$ .

## ACKNOWLEDGMENTS

We thank T. Piran for helpful discussions. This work was supported in part by 973 Programme of China (No. 2013CB837000 and No. 2014CB845800), by NSFC under grants 11525313 (the National Natural Fund for Distinguished Young Scholars), 11273063 and 11433009, by the Chinese Academy of Sciences via the Strategic Priority Research Program (No. XDB23040000) and the External Cooperation Program of BIC (No. 114332KYSB20160007).

## REFERENCES

- Abadie, J., Abadie, J., Abbott, B. P., et al. 2010, *CQGra*, 27, 173001.
- Abbott, B. P. et al. (LIGO Scientific Collaboration and Virgo Collaboration), 2016, *ApJL*, 832, L21.
- Aloy, M. A., Janka, H.-T., & Müller, E. 2005, *A&A*, 436, 273.
- Baiotti, L., & Rezzolla, L. 2017, *RPPH*, 80, 096901
- Barnes, J. & Kasen, D. 2013, *ApJ*, 773, 18.
- Barthelmy, S. D., Baumgartner, W. H., Beardmore, A. P., et al. 2015, *GCN Circ*, 17761, 1
- Beardmore, A. P., Page, K. L., Palmer, D. M., & Ukwatta, T. N. 2015, *GCN Circ*, 17743, 1
- Berger, E., 2014, *ARA&A*, 52, 43
- Berger, E., et al. 2003, *Nature*, 426, 154.
- Berger, E., Fong, W., & Chornock, R. 2013, *ApJL*, 744, L23
- Castro-Tirado, A. J., Sanchez-Ramirez, R., Lombardi, G., & Rivero, M. A. 2015, *GCN Circ*, 17758, 1
- Clark, J. P. A. & Eardley, D. M. 1977, *ApJ*, 215, 311.
- Coward, D. M., Howell, E. J., Piran, T., et al. 2012, *MNRAS*, 425, 2668
- Clark, J., Evans, H., Fairhurst, S., et al. 2015, *ApJ*, 809, 53
- Dai, Z. G., & Gou, L. J., 2001, *ApJ*, 552, 72.
- Dominik, M., Berti, E., OShaughnessy, R., et al. 2015, *ApJ*, 806, 263
- Eichler D., Livio M., Piran T., & Schramm D. N. 1989, *Natur*, 340, 126
- Evans, P. A., Beardmore, A. P., Page, K. L., et al. 2009, *MNRAS*, 397, 1177
- Fan, Y. Z., Yu, Y. W., & Xu, D. et al. 2013, *ApJL*, 779, L25
- Fan, Y. Z., Wei, D. M., Zhang, F. W., & Zhang, B. B. 2012, *ApJ*, 751, 49
- Fong, W., Berger, E., Margutti, R., et al. 2012, *ApJ*, 756, 189
- Fong, W., & Berger, E., 2013, *ApJ*, 776, 18
- Fong, W., Berger, E., Metzger, B. D., et al. 2014, *ApJ*, 780, 118
- Fong, W., Berger, E., Margutti, R., & Zauderer, B. A. 2015, *ApJ*, 815, 102.
- Frail, D. A., Kulkarni, S. R., Sari, R. et al. 2001, *ApJ*, 562, L55
- Gehrels, N., Norris, J. P., Barthelmy, S. D., et al. 2006, *Natur*, 444, 1044
- Golenetskii, S., Aptekar, R., Prederiks, D., et al. 2015, *GCN Circ*, 17752, 1
- Gottlieb, O., Nakar, E., & Piran, T. 2017, *arXiv:1705.10797*
- Guetta, D., & Piran, T. 2005, *A&A*, 435, 421
- Hotokezaka, K., Kyutoku, K., Tanaka, M. et al. 2013, *ApJL*, 778, L16.
- Hotokezaka, K. et al. 2013, *Phys. Rev. D*, 87, 024001.
- Huang, Y. F., Cheng, K. S., & Gao, T. T. 2006, *ApJ*, 637, 873.
- Jeong, S., Park, I. H., Hu, Y., et al. 2016, *GCN Circ*, 19847, 1
- Jin, Z. P., Yan, T., Fan, Y. Z., & Wei, D. M., 2007, *ApJL*, 656, L57.
- Jin, Z. P., et al. 2015, *ApJL*, 811, L22
- Jin, Z. P., et al. 2016, *Nat. Commun.*, 7, 12898
- Kann, D. A., Tanga, M., & Greiner, J. 2015, *GCN Circ*, 17757, 1
- Kasliwal, Mansi M., Korobkin, Oleg, Lau, Ryan M., Wollaeger, Ryan, & Fryer, Christopher L. 2017, *ApJ*, 843, L34
- Knust, F., Greiner, J., van Eerten, J. H., et al. 2017, *arXiv:1707.01329*
- Kochanek, C. S., & Piran, T. 1993, *ApJL*, 417, L17
- Kouveliotou, C., Meegan, C. A., Fishman, G. J., et al. 1993, *ApJL*, 413, L101
- Kulkarni, S. R. 2005, *arXiv:astro-ph/0510256*
- Kumar, P., & Granot, J., 2003, *ApJ*, 591, 1075.
- Kumar, P., & Zhang, B., 2015, *PhR*, 561, 1
- Lü, J., Zou, Y.-C., Lei, W.-H., et al. 2012, *ApJ*, 751, 49
- Lattimer, J. M. *Annu. 2012, Rev. Nucl. Part. Sci.*, 62, 485.
- Lattimer, J. M., & Prakash, M. 2016, *Phys. Rep.*, 621, 127-164.
- Lazzati, D., Deich, A., Morsony, B. J., Workman, J. C. 2017, *MNRAS*, 471, 1652
- Levan, A. J., Wiersema, K., Tanvir, N. R., et al. 2016, *GCN Circ*, 19846, 1
- Li, L.-X., & Paczyński, B. 1998, *ApJL*, 507, L59
- Li, X. et al. 2016, *ApJ*, 827, 75
- Li, X. et al. 2017, *ApJL*, 844, L22
- Liang, E.-W., Yi, S.-X., Zhang, J., et al. 2010, *ApJ*, 725, 2209
- Marshall, F. E., & Beardmore, A. P. 2015, *GCN Circ*, 17751, 1
- Meegan, C., et al. 2009, *ApJ*, 702, 791
- Metzger, B. D., Martínez-Pinedo, G., Darbha, S. et al. 2010, *MNRAS*, 406, 2650
- Murguía-Berthier, A., Ramirez-Ruiz, E., Montes, G., et al. 2017, *ApJL*, 835, L34
- Nagakura, H., Hotokezaka, K., Sekiguchi, Y., Shibata, M., & Ioka, K., 2014, *ApJL*, 784, L28
- Nakar, E. 2007, *Phys. Rep.* 442, 166.
- Nicuesa Guelbenzu, A., Klose, S., Rossi, A., et al. 2011, *A&A*, 531, L6
- Paczynski, B. 1990, *ApJ*, 363, 218
- Palmer, D. M., Barthelmy, S. D., & Cummings, J. R. 2016, *GCN Circ*, 19844, 1
- Pannarale, F., & Ohme, F. 2014, *ApJL*, 791, L7.
- Paschalidis, V. 2017, *Classical and Quantum Gravity*, 34, 084002.
- Perley, D. A., & McConnell, N. J. 2015, *GCN Circ*, 17745, 1
- Piran, T. 2004, *RvMP*, 76, 1143
- Planck Collaboration, Ade, P. A. R., Aghanim, N., Armitage-Caplan, C., et al. 2014, *A&A*, 571, 16
- Rhoads, J. E. 1999, *ApJ*, 525, 737.
- Rossi, E., Lazzati, D. & Rees, M. J., 2002, *MNRAS* 332, 945.
- Sari, R., T. Piran, & Halpern, J. P. 1999, *ApJL*, 519, L17.
- Siegel, M. H. Barthelmy, S. D., Burrows, D. N., et al. 2016, *GCN Circ*, 19833, 1
- Siellez, K., Boer, M., Gendre, B., & Regimbau, T. 2016, *arXiv:1606.03043*
- Soderberg, A. M., Berger, E., Kasliwal, M., et al. 2006, *ApJ*, 650, 261
- Stanbro, M., & Meegan, C. 2016, *GCN Circ*, 19843, 1
- Tanaka, M., & Hotokezaka, K. 2013, *ApJ*, 775, 113
- Tanaka, M., Hotokezaka, K., Kyutoku, K. et al., 2014, *ApJ*, 780, 31.
- Tanvir, N. R., Levan, A. J., Fruchter, A. S. et al. 2013, *Natur*, 500, 547
- Tanvir, N. R., Levan, A. J., Fruchter, A. S., et al. 2015, *GCN Circ*, 18100, 1
- Troja, E., Sakamoto, T., Cenko, S. B., et al. 2016a, *ApJ*, 827, 102.
- Troja, E., Tanvir, N., Cenko, S. B., et al. 2016b, *GCN Circ*, 20222, 1
- Villasenor, J. S., Lamb, D. Q., Ricker, G. R., et al. 2005, *Natur*, 437, 855
- Williamson, A. R., Biwer, C., Fairhurst, S., et al. 2014, *PhRvD.*, 90I2004
- Wei, D. M., & Jin, Z. P., 2003, *A&A*, 400, 415.
- Woosley, S. E.; Bloom, J. S. 2006, *ARA&A*, 44, 507
- Wu, X. F., Dai, Z. G., Huang, Y. F., & Lu, T. 2005, *MNRAS*, 357, 1197.
- Xu, D., Starling, R. L. C., Fynbo, J. P. U. et al. 2009, *ApJ*, 696, 971
- Xu, D., Malesani, D., de Ugarte Postigo A., et al. 2016, *GCN Circ*, 19834, 1
- Yang, B., Jin, Z. P., Li, X. et al. 2015, *Nat. Commun.*, 6, 7323
- Zhang, B., & Mészáros, P. 2002, *ApJ*, 571, 876.
- Zhang, B., Dai, X., Lloyd-Ronning, N. M., & Mészáros, P. 2004, *ApJL*, 601, L119
- Zhang, B., & Mészáros, P. 2004, *IJMPA*, 19, 2385
- Zhang, F.-W., Shao, L., Yan, J.-Z., & Wei, D.-M. 2012, *ApJ*, 750, 88
- Zhang, S., Jin, Z. P., Wang, Y. Z., & Wei, D. M. 2017, *ApJ*, 835, 73.